The North American Land Data Assimilation System (NLDAS)

Kenneth Mitchell and Dag Lohmann

NCEP/EMC, Camp Springs, MD 20746
United States
Kenneth.Mitchell@noaa.gov

ABSTRACT

This paper describes the purpose, approach, configuration, results, validation and plans of the uncoupled North American Land Data Assimilation System (NLDAS). NLDAS is a multi-institution partnership of three U.S. federal agencies and five universities to develop a realtime and retrospective uncoupled land data assimilation system on a 1/8° grid over the continental U.S. (CONUS) and consists of a) four land models executing in parallel in uncoupled mode, b) common hourly surface forcing and c) common streamflow routing. This initiative is largely sponsored by the GCIP/GAPP program of GEWEX. This paper describes and evaluates the 3-year NLDAS execution of 01 Oct 96 to 30 Sep 99 – a period rich in observations for validation. The validation includes a) mesoscale observing networks of land surface forcing, fluxes and states, b) regional snowpack measurements, c) daily streamflow measurements and d) satellite-based retrievals of snow cover, land-surface skin temperature (LST) and surface insolation. The results show substantial inter-model differences in surface evaporation and runoff (especially over non-sparse vegetation), soil moisture storage, snowpack and LST. Owing to surprisingly large inter-model differences in aerodynamic conductance, inter-model differences in mid-day summer LST were unlike those expected from the inter-model differences in Bowen ratio. Lastly, results of experiments to assimilate LST in one of the four land models are presented, including assessment and assimilation of geostationary satellite-derived LST.

1. Introduction

For two decades, advances in providing atmospheric initial states via 4-dimensional data assimilation (4DDA) have paved the way for emerging 4DDA systems for the ocean and land. The backbone of any 4DDA system is the geophysical model whose execution provides temporally and spatially continuous background states, into which generally discontinuous observations are assimilated from various observing platforms (in situ, satellite, radar). A land data assimilation system (LDAS) is needed to blend sparse land observations with the background fields of a land surface model (LSM). The accuracy of the LSM background field (and companion surface and sub-surface water/energy fluxes) is crucial to LDAS viability. The chief objective of the NLDAS study presented here is to generate and validate, over a 3-year period over the CONUS domain, the background land states and surface fluxes of four LSMs: Noah, Mosaic, VIC, and Sacramento – denoted SAC.

Coupled land-atmosphere 4DDA systems (including global reanalysis) often yield significant errors and drift in soil moisture/temperature and surface energy/water fluxes, owing to substantial biases in the surface forcing from the parent atmospheric models. To constrain such errors and drift, coupled land-atmosphere 4DDA systems often nudge the soil moisture according to 1) climatology of soil moisture, 2) differences between the observed and 4DDA background fields of precipitation or 3) screen-level air temperature and dew point errors. Such nudging methods, however, do not reduce the main error source, namely large bias in the land surface forcing (especially precipitation and solar insolation) of the parent atmospheric model.

The NLDAS here omits soil moisture nudging in favor of using non-model, observation-based precipitation analyses and non-model, satellite-based surface insolation fields (with all other surface forcing from atmospheric 4DDA) to drive the four participating LSMs, all with common hourly surface forcing on a 1/8° grid over the CONUS domain. Specifically, the NLDAS project achieved the following key objective: 1) to develop and execute the first realtime prototype of a continental-scale uncoupled land 4DDA backbone

(continuously cycled land-model states) executed daily at NCEP using realtime streams of hourly to daily data, and 2) develop and execute a companion retrospective mode for research.

The present paper briefly surveys the NLDAS results from the ten joint NLDAS papers listed below, which appear in the recent GCIP-3 Special Issue of the Journal of Geophysical Research. Henceforth here, each paper below is cited by the given 3-letter label, denoting last initial of first two authors and N for NLDAS.

Mitchell et al. (2004)	ML-N	NLDAS overview, summary of results from next nine papers
Cosgrove et al. (2003a)	CL-N:	generation of land surface forcing
Luo et al. (2003)	LR-N:	validation of land surface forcing
Pinker et al. (2003)	PT-N:	production/validation of GOES-based solar insolation
Lohmann et al. (2004)	LM-N:	production/validation of streamflow and water budget
Robock et al. (2003)	RL-N:	validation of energy budget, soil moisture/temperature
Schaake et al. (2004)	SD-N:	evaluation of soil moisture storage and range
Sheffield et al. (2003)	SP-N:	validation of simulated snow cover
Pan et al. (2003)	PS-N:	validation of simulated snowpack content
Cosgrove et al. (2003b)	CM-N:	evaluation and testing of spin-up

For brevity, the reference list herein gives only Mitchell et al. (2004), which contains the full citations of the other nine papers above and a list of all acronyms used here. The NLDAS collaborating institutions/PIs include NCEP/EMC (K. Mitchell), NASA/GSFC (P. Houser), NWS/OHD (J. Schaake), NESDIS/ORA (J. D. Tarpley), NCEP/CPC (R. W. Higgins), Princeton University (E. Wood), Rutgers University (A. Robock), and the Universities of Maryland (R. Pinker), Washington (D. Lettenmaier), and Oklahoma (K. Crawford).

2. NLDAS Configuration

The NLDAS is executed over a rectangular 1/8° grid that encompasses the continental U.S. (CONUS). Across the four LSMs, NLDAS applies a common land mask, terrain elevation, hourly surface forcing, soil texture and vegetation classes, streamflow routing, and frequency (hourly) and format (GRIB) of model input/output. Of the four LSMs, two use tiling (Mosaic for vegetation, VIC for vegetation and elevation). SAC omits treatment of vegetation. Though the LSMs apply common fields of vegetation and soil class, the NLDAS partners chose NOT to impose common vegetation and soil properties, such as 1) parameter values, 2) geometry of soil layers and root zone or 3) seasonal phenology, to avoid disrupting legacy of calibrations.

The NLDAS control runs here required initial values of all LSM state variables for the common start time of 00 UTC on 01 Oct 96. Initial snowpack was set to zero (reasonable for 01 Oct over the NLDAS domain). Initial soil moisture and temperature were derived from the soil states of the NCEP/DOE Global Reanalysis 2 for 01 Oct 96. The soil moisture was provided to each LSM as a vertically uniform percent of saturation, which each LSM converted to its own absolute moisture state via its own parameters. CM-N examined the spin-up in all four LSMs and found that, for practical purposes, the spin-up required about one year.

The sources, generation and validation of NLDAS surface forcing, which is produced in realtime and retrospectively, is summarized in ML-N and presented in detail in LR-N, CL-N, PT-N, and PS-N. The nine forcing fields required by the four LSMs are: U/V 10-m wind components, 2-m air temperature and specific humidity, surface pressure, downward longwave and shortwave radiation, and convective and total precipitation. SAC requires only total precipitation (*P*), air temperature and potential evaporation (*PE*). In NLDAS, SAC uses the *PE* computed by the Noah LSM. Only Mosaic requires convective precipitation. Except for precipitation and solar insolation, the source of NLDAS forcing is NCEP's Eta model-based Data Assimilation System (EDAS), a 3-hourly, continuously cycled, N. American mesoscale 4DDA system. To

account for NLDAS vs. EDAS surface-elevation differences, a terrain-height adjustment is applied to the air temperature and surface pressure using a standard lapse rate (6.5 K km^{-1}), then to specific humidity (keeping relative humidity fixed) and downward longwave radiation (using new air temperature, specific humidity). CL-N details the spatial/temporal interpolations and terrain-height adjustment. The NLDAS precipitation forcing is anchored to NCEP's 1/4° gage-only daily precipitation analyses, which utilize about 6500 (realtime) or 13000 (retrospectively) gauge observations of daily precipitation. In NLDAS, this daily analysis is interpolated to 1/8°, and then disaggregated to hourly (details in CL-N) via temporal weights derived from hourly, radar-based (WSR-88D) precipitation fields. This hourly disaggregation preserves the gauge-based daily precipitation. Lastly, convective precipitation is estimated by multiplying NLDAS total precipitation by the ratio of EDAS convective to EDAS total precipitation. There is no distinction between rainfall and snowfall in NLDAS precipitation forcing. This requires criteria to infer snowfall. The input precipitation at each model time step is assumed to be all rainfall for surface air temperature > 0°C and all snowfall otherwise. The NLDAS surface solar insolation forcing is obtained from hourly, 1/2° GOES satellite-derived solar insolation, as described and validated in PT-N, LR-N and CL-N.

Key references and the attributes of the Noah, VIC, Mosaic and SAC LSMs in NLDAS are summarized in ML-N. Of the many LSMs, these four give a good cross-section of different traditions of application, including small scale versus large scale, coupled versus uncoupled, distributed versus lumped, with explicit vegetation (Noah, VIC, Mosaic) versus without (SAC), and tiled (Mosaic and VIC) versus non-tiled (Noah and SAC). Mosaic and Noah emerged from the surface-vegetation-atmosphere transfer (SVAT) setting of coupled atmospheric modeling with little calibration. VIC and SAC grew from the hydrology community as uncoupled hydrology models with considerable calibration. VIC was developed as a macro-scale semi-distributed model. SAC was developed as a lumped conceptual hydrology model, highly calibrated for small catchments and used operationally in NWS River Forecast Centers. Subsequent to their early heritage, Mosaic, Noah, and VIC have been widely executed in coupled and uncoupled modes from small to large scales and all three can be considered as SVATs. As such, Mosaic, Noah and VIC simulate LST, the surface energy and water balance, snowpack, and soil moisture in several soil layers (4 in Noah, 3 in VIC and Mosaic). All three SVATs include direct evaporation from soil, transpiration from vegetation, evaporation of interception, and snow sublimation; and all explicitly model canopy resistance, though their formulations differ, as does their vegetation phenology and root profiles. Only Noah simulates soil freezing and thawing. In all three SVATs, the surface infiltration schemes account for subgrid variability in soil moisture and precipitation, but the treatments differ. In contrast, SAC is a conceptual rainfall-runoff, storage-type model. It treats only the surface water budget, omitting the surface energy budget, and uses the snowpack model of called SNOW17. SAC outputs evaporation E and runoff, with E being a fraction of input PE. The NWS Office of Hydrological Development (OHD) recently developed a distributed (non-lumped) version of SAC with a priori un-calibrated parameters intended for testing from small basins to entire continents. NLDAS provides the first tests of the distributed SAC model at continental scales. These are pilot tests, as SAC lacks the legacy of continental testing of the other 3 LSMs. SAC calibration was omitted in NLDAS runs and its primary parameters were specified a priori.

LM-N presents the formulation of the common streamflow model in NLDAS and validates the daily streamflow simulations of the four LSMs over 9 large basins and 1145 small to medium-sized (and mostly unregulated) basins across the CONUS using USGS streamflow measurements. The streamflow routing requires both a river network (flow-direction mask) on the NLDAS grid and a routing model. The chosen routing model is linear and calculates the timing of the runoff reaching the grid-cell outlet, as well as the transport of water through the river network. It operates in two modes: 1) distributed, using a-priori grid-cell specific routing parameters common to all four models and 2) "lumped", in which constant routing parameters were separately calibrated for each of the 1145 basins, yielding a separately calibrated unit

hydrograph for each basin for each model. A cool season impact on the modeled runoff is the timing of snowmelt in each LSM. LM-N found streamflow performance increasingly degraded in regions of increased seasonal snowfall. The worst cases of peak streamflow timing occurred in the snow season of the mountain ranges of northwest CONUS, where the LSMs differed by up to four months in their peak-flow timing.

3. Assessment of the NLDAS water budget

We summarize here the assessment by LM-N of the NLDAS water budget. We begin with the annual budget for the period 01 Oct 97 to 30 Sep 99. Over one or more annual cycles, mean annual storage change (soil moisture, snowpack, etc.) is negligible and thus the annual surface water budget is well approximated by $P = E + R$, wherein P, E, and R denote the mean annual totals of precipitation, evaporation, and runoff, respectively. Thus, the difference of the observed values of mean annual P and R (from observed streamflow) yields an observation-based estimate of mean annual E. LM-N performed this analysis for NLDAS and derived Figure 1, which shows how each NLDAS LSM partitioned the observed and prescribed mean annual P into mean annual E and R over four CONUS quadrants. In Figure 1a, each diagonal denotes the mean-annual area-averaged precipitation of a given quadrant (given by the diagonal's x- or y-axis intercept value). On each diagonal, each LSM's symbol projected onto the x-axis (y-axis) yields that LSM's quadrant-average mean annual runoff (evaporation). The tiny displacement of an LSM's symbol from the diagonal represents the negligible change in that LSM's total water storage over the period. The disparity in mean annual E and R among the LSMs in Figure 1a is striking over the well vegetated, eastern half of the CONUS. ML-N illustrates this disparity in CONUS-wide maps of evaporation and runoff for each LSM. Noah and VIC have notably lower evaporation and hence higher runoff than Mosaic and SAC. Large disparity among LSMs in E vs. R partitioning was noted in PILPS and GSWP.

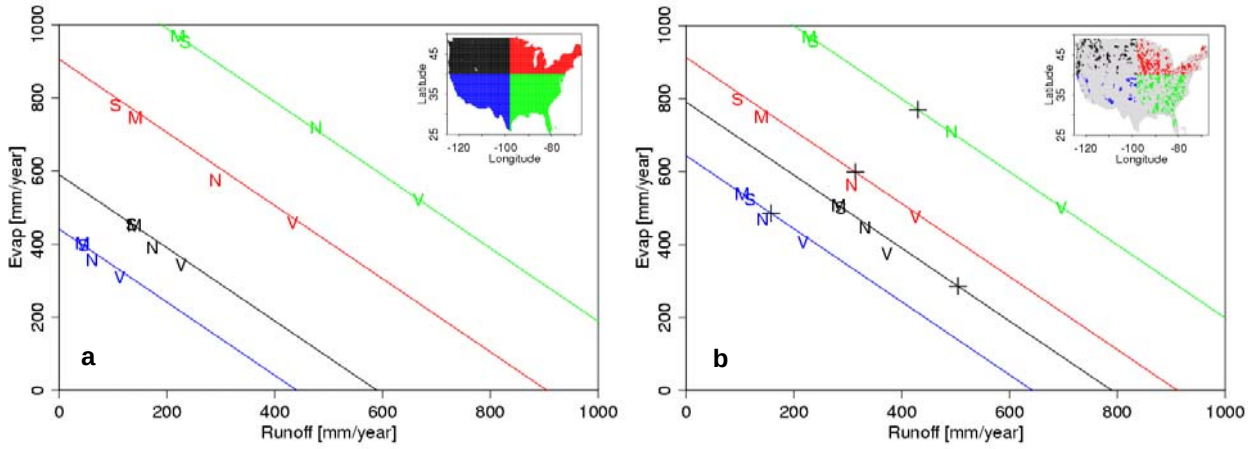

Figure 1(a) Partitioning of area-mean mean annual precipitation (diagonal, mm/year) into area-mean mean annual runoff (x-axis, mm/year) and evaporation (y-axis, mm/year) for the CONUS quadrants (inset) of Southeast-SE (top diagonal), Northeast-NE (2nd diagonal), Northwest-NW (3rd diagonal) and Southwest-SW (bottom diagonal) by Noah (N), VIC (V), Mosaic (M), and SAC (S) for 01 Oct 97 to 30 Sep 99. (b) As in (a), except area-mean is for sub-area of basin-set depicted in inset for each quadrant. "+" symbol depicts observed area-mean mean annual runoff.

The partitioning can be validated over the sub-regions of the quadrants for which basin-observed streamflow is available. Figure 1b, which utilizes USGS-observed streamflow from 1145 assessment basins, is the counterpart to Figure 1a obtained by area averaging the observed precipitation and LSM simulated evaporation and runoff only over the quadrant sub-area spanned by these basins (Figure 1b inset). For each basin, observed streamflow (m^3s^{-1}) is converted to mean-annual total discharge (m^3), in turn converted (using the basin area) to area-average mean-annual runoff (mm) for the basin. The "+" symbol in Figure 1b depicts the area-mean of this observed runoff over the same quadrant sub-area. Projecting the "+" symbol onto the y-axis yields the budget-based estimate of the area-average mean annual evaporation. The reliability of this

observation-based evaporation estimate depends on the reliability of both the observed streamflow (high reliability) and the NLDAS precipitation forcing. Over NE and SE, which manifest relatively flat terrain and good density of precipitation gages, we trust the precipitation analysis and the estimates of evaporation there. For NE and SE, one sees in Figure 1b that evaporation and runoff of Noah are close to observed, while Mosaic and SAC show large biases of high evaporation and low runoff, with VIC yielding the reverse. In the NW and SW, owing to rugged orography and sparseness of both precipitation gauges and unregulated basins, the reliability of the observation-based evaporation and runoff estimates is rather uncertain.

Figure 2 gives the time series of area-average monthly evaporation *E* for each CONUS quadrant for the NLDAS LSM control runs, including the initial spin-up year. We focus on the more humid eastern quadrants, which show the most disagreement. There, during mid and late summer, Mosaic clearly has the highest evaporation during mid-to-late summer, while SAC has the highest in winter and spring. Noah evaporation generally falls between that of Mosaic and VIC in the warm season. VIC has the lowest evaporation in virtually every month in the vegetated eastern quadrants, consistent with the earlier annual results. Figures 2b,d strongly suggest that Mosaic and VIC manifest rather different canopy conductance. Such large differences in warm season evaporation imply large warm season differences in soil moisture storage change. To examine this, Figure 3 shows the time series of area-average monthly-mean total column soil moisture for all four quadrants for the 3 LSMs that carry explicit soil layers. After year one, spin-up is essentially complete. For years 2-3, Figure 3 together with Figures 1-2 reveal 1) very different levels of total soil moisture across the LSMs, 2) somewhat more similarity, yet still significant differences, in annual-cycle amplitude (seasonal change) of total soil moisture among the LSMs, 3) larger differences among the models over the wetter eastern quadrants than the drier western quadrants, 4) that the model with the highest level of soil moisture is not the model with the largest evaporation or seasonal change in soil moisture. Further analysis in ML-N shows that Mosaic's large warm season evaporation in non-arid areas compared to Noah and VIC stems from its notably more vigorous upward diffusion of soil moisture from below the root zone.

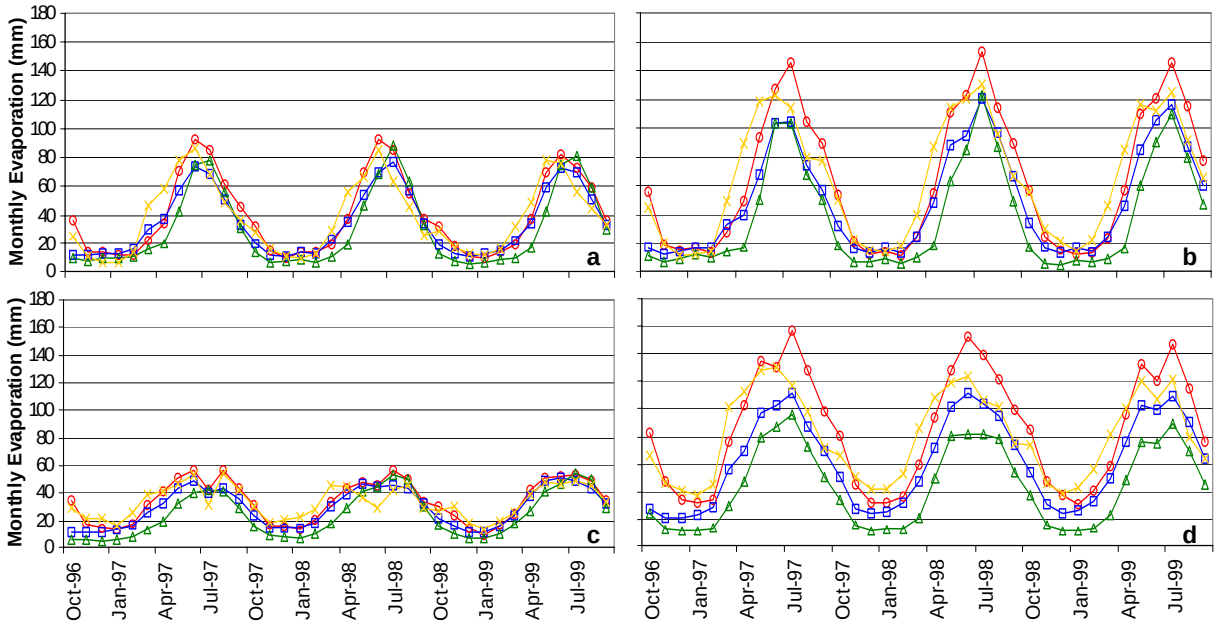

Figure 2 Time series of area-averaged monthly evaporation (mm/month) in NLDAS for Noah (squares), VIC (triangles) Mosaic (circles), and SAC (crosses) over the four CONUS quadrants of (a) NW, (b) NE, (c) SW and (d) SE for Oct 96 to Sep 99.

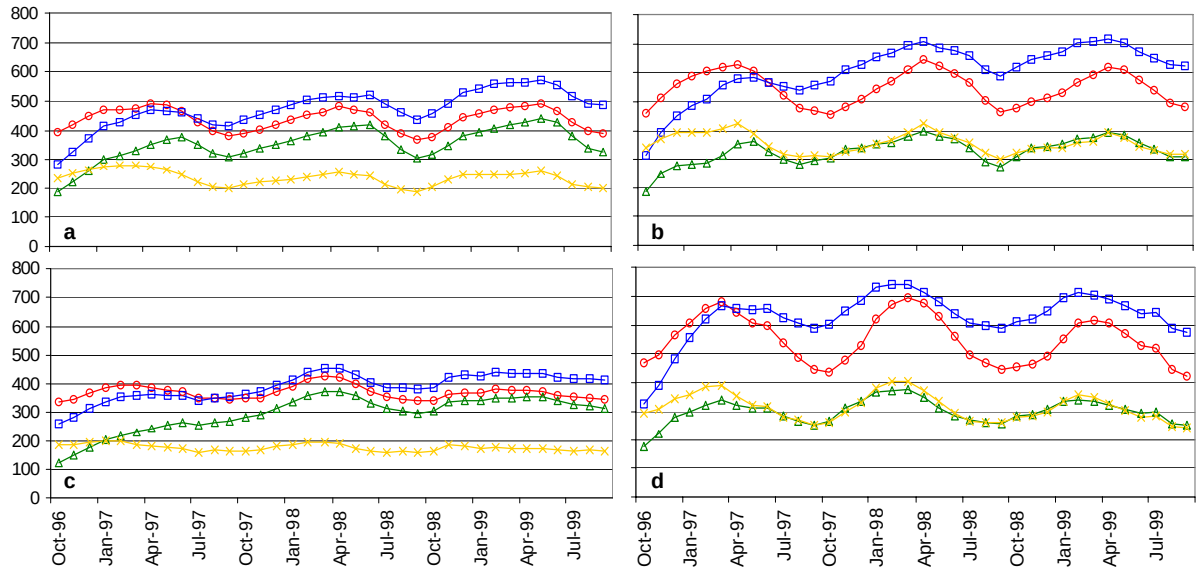

Figure 3 Time series of area-averaged monthly mean total column soil moisture (mm) in NLDAS for Noah (squares), VIC (triangles), Mosaic (circles), and SAC (crosses) for the CONUS quadrants of (a) NW, (b) NE, (c) SW and (d) SE for Oct 96 to Sep 99.

Figure 4, from the study of SD-N, compares NLDAS bi-monthly area-mean 2-m soil moisture with that from 17 measurement sites across the state of Illinois, from of the Illinois State Water Survey. For VIC, separate best-fit lines for northwest and southeast Illinois were required, because past VIC calibration yielded rather different soil moisture storage capacities in these regions. In Figure 4, Mosaic shows a dynamic storage range greater than the other LSMs and about 50% more than observed, owing to larger warm season depletion. Noah and SAC agree with observations in both storage range and storage magnitude. VIC also shows good storage range over its two regions, but storage magnitude lower than observed. The study of RL-N found similar contrasts in soil moisture character between LSMs and between observations and LSMs using measured soil moisture from the Oklahoma Mesonet, including scrutiny at individual stations. RN-L also presents revealing sensitivity tests of the SVAT models at individual soil moisture measuring stations.

Turning to snowpack issues, the studies by PS-N and SP-N perform large-scale assessment of NLDAS snowpack water equivalent (SWE) and snow cover extent (SCE), respectively. SP-N validated NLDAS snow-cover simulations against the NESDIS daily, N. Hemisphere, 24-km snow cover analysis and found substantial differences across the LSMs, arising from differences in LSM treatment of snow cover fraction, snow albedo, and snow sublimation. PS-N validated NLDAS SWE simulations against 110 western SNOTEL stations, which measure SWE, air temperature and precipitation every 15 minutes. The majority of SNOTEL elevations are above 1000 m, with mean elevation near 2500 m. Figure 5 shows model versus observed mean-annual maximum SWE for the control runs of the four LSMs (and two VIC sensitivity tests) at the SNOTEL sites. All the LSMs substantially underestimate annual maximum SWE. Noah has the largest low bias and the lowest correlation. Mosaic also shows a rather low correlation. SAC and VIC have notably better bias and substantially higher correlation. The model with elevation tiling (VIC) yields the highest correlation, yet the simplest model (SAC) without elevation tiling or energy balance treatment is closely competitive. PS-N found the NLDAS precipitation forcing to be biased substantially low when compared to observed precipitation at the SNOTEL sites. PS-N executed two tests in VIC with two methods of bias-corrected precipitation. The results are shown in Figures 5e,f and discussed in PS-N. Given bias-corrected precipitation forcing, VIC snowpack simulations manifested little bias in mean-annual maximum SWE. The rather poor performance of Noah snowpack simulations prompted considerable changes to Noah snowpack physics, including the treatments of snow cover fraction and snow albedo and a reformulation of Noah sublimation over patchy snow cover. These changes yielded marked improvement (not shown).

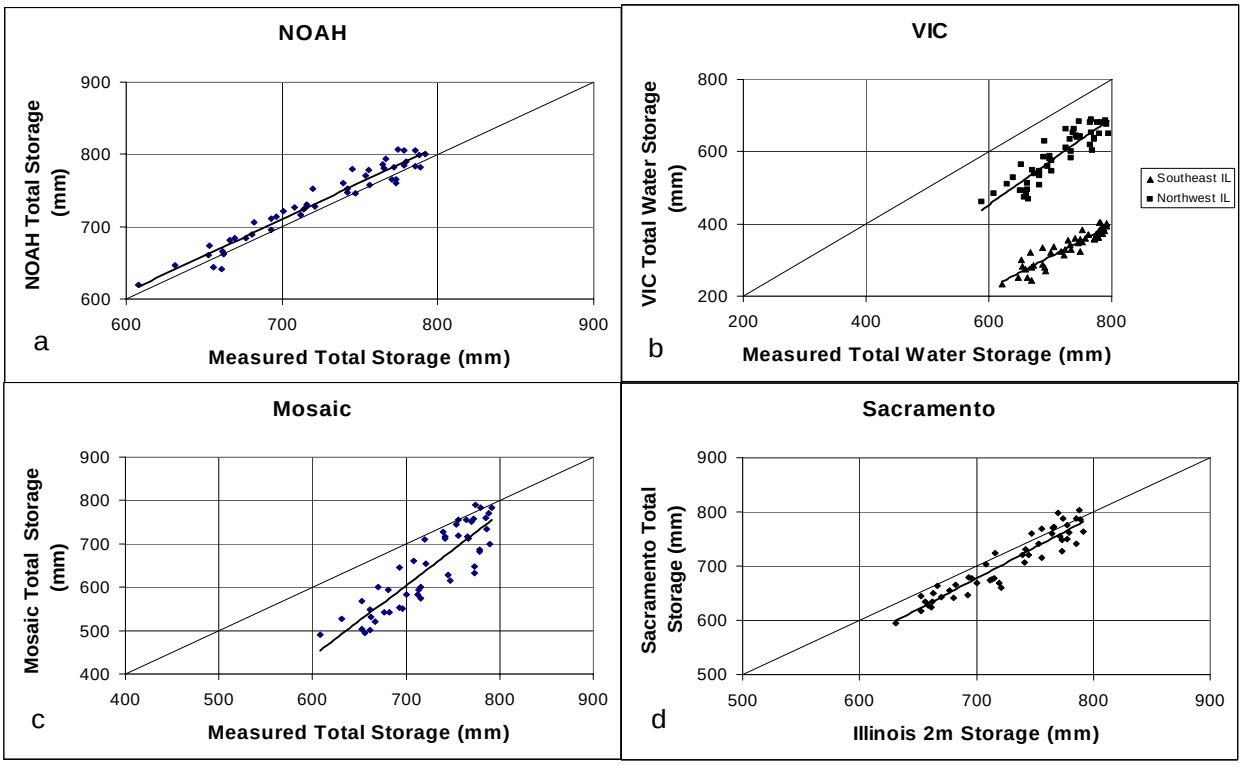

Figure 4 Two-year comparison of NLDAS versus observed bi-monthly total soil moisture (mm) in top 2 m, averaged over 17 sites across Illinois during Oct 97 to Sep 99 for (a) Noah, (b) VIC, (c) Mosaic, and (d) SAC. Note different axis ranges. Text describes the two sets in (b)

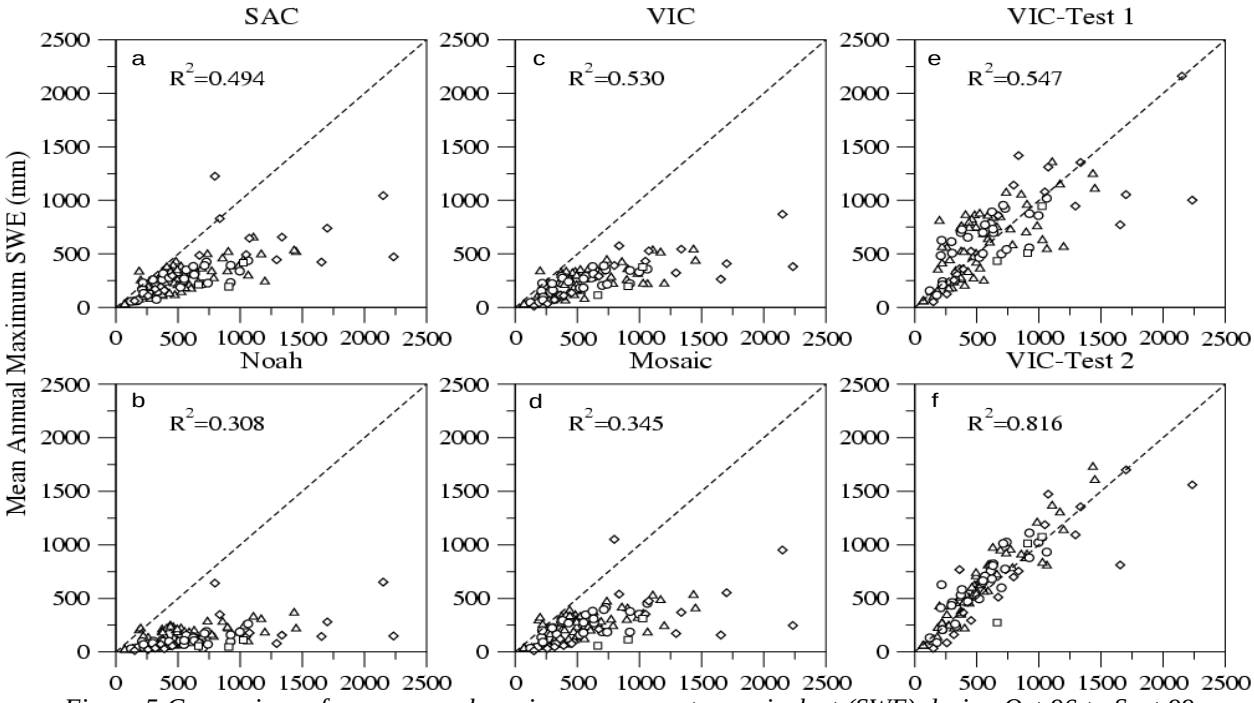

Figure 5 Comparison of mean annual maximum snow water equivalent (SWE) during Oct 96 to Sept 99 between observations (x-axis) and model simulations (y-axis) at 110 SNOTEL sites for the control runs of (a) SAC, (b) Noah, (c) VIC and (d) Mosaic, and two VIC tests runs forced with regionally corrected precipitation forcing (e) and locally corrected precipitation forcing (f).

4. Validation of NLDAS surface energy fluxes and LST

This section presents results from the validation of NLDAS surface energy fluxes in the study by RL-N, which validates energy fluxes during Jan 98 to Sep 99 using the 24 extended facility (EF) flux stations of the

ARM/CART network in Oklahoma and Kansas. The results omit the SAC, as SAC omits the physics of surface energy balance. Multi-station spatial averaging and hourly temporal averaging are used to reduce the influence of scale differences between NLDAS grid cells and point-wise flux stations. Figure 6 shows the 21-month time series of monthly-mean observed versus modeled surface fluxes of the NLDAS control runs, including net radiation (*R*), latent heat flux (*LE*), sensible heat flux (*H*), and ground heat flux (*G*). As anticipated from the results for the NE and SE quadrants in Figure 1, Mosaic has a substantial high bias in *LE* and, correspondingly, a substantial low bias in *H*. VIC has a substantial low bias in *LE* and high bias in *H* throughout most of the year (except spring), while Noah shows much smaller bias in *LE* (slightly low in warm season) and *H* (modestly high in warm season). The counterpart to evaporation bias in Figure 1b was runoff bias of opposite sign. Here the counterpart to LE bias is sensible heat flux bias of opposite sign.

Figure 6 shows serious errors in monthly mean ground heat flux in Mosaic. Noah shows comparatively little error in ground heat flux. Other figures (not shown) from RL-N and ML-N also show large ground heat flux errors on hourly time scales throughout much of the mean diurnal cycles of both Mosaic and VIC. VIC's daytime and nighttime biases in *G* are rather symmetric and opposite in sign and thus nearly cancel on the monthly mean scale of Figure 6. Both Mosaic and VIC show large daytime diurnal high bias and phase error in G. Finally, the simultaneous and very high daytime biases in *G* and *LE* in Mosaic during Apr-Jun conspire to yield dramatically low sensible heat flux (*H*) during these months in Figure 6. The poor ground heat flux performance of Mosaic and VIC prompted sensitivity runs in NLDAS, as reported in RL-N and ML-N, wherein the surface heat capacity parameters in both models were changed, yielding in dramatic improvement in the ground heat flux of both models. However, the improvement in *G* in the Mosaic and VIC sensitivity tests provided no improvement in the large warm-season *LE* biases in Mosaic or VIC in Figure 6. Rather, the increase in daytime available energy (*R-G*) gained by reducing daytime high bias in *G*

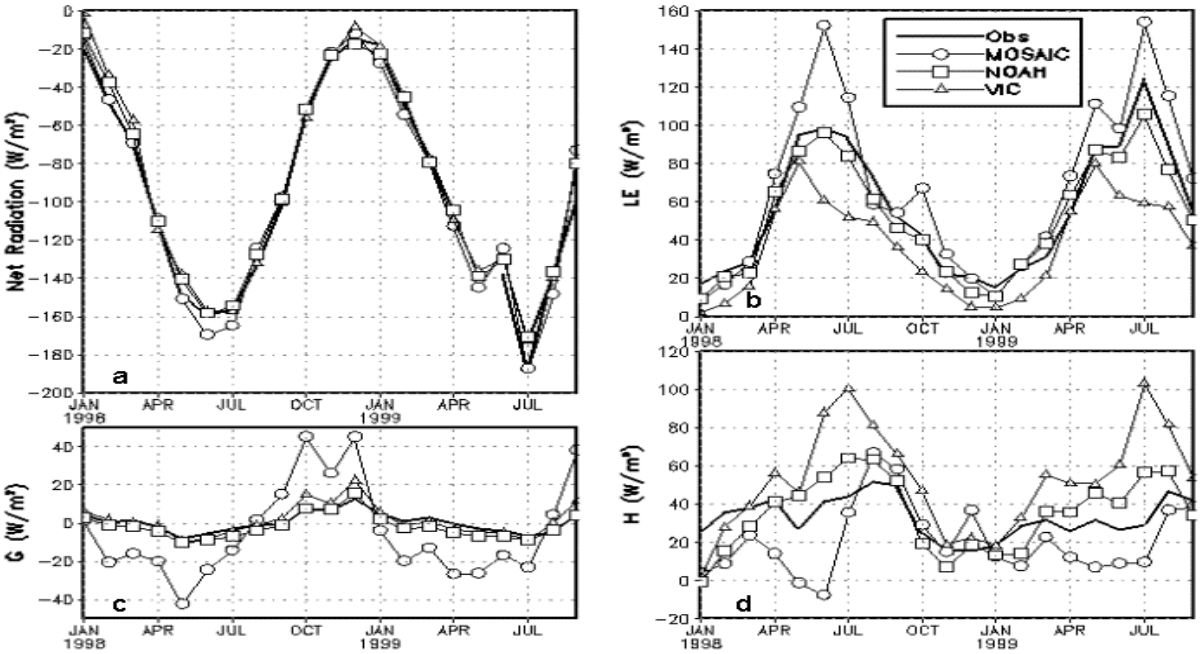

Figure 6 Time series of monthly mean surface energy fluxes (Wm-2) of (a) net radiation R, (b) latent heat LE, (c) ground heat G and (d) sensible heat H averaged over the ARM/CART sites during Jan 98 to Sep 99 from observations (bold line, no symbols) and control runs for Noah (squares), VIC (triangles), and Mosaic (circles). Positive flux is heat sink to surface except in G.

acted only to increase the sensible heat flux *H*, in both models, which helped the low *H* bias in Mosaic and worsened the high *H* bias in VIC. The non-responsiveness of *LE* and the high response in *H* strongly suggests that the canopy resistance is substantially higher than the aerodynamic resistance in both models in

this vegetated region in the warm season. Sensitivity tests of canopy resistance will be a focus in all three SVAT models in NLDAS follow-on studies.

A chief goal of NLDAS is assimilation of satellite data to improve soil moisture, and in turn, surface fluxes. One keen interest is the assimilation of satellite-derived LST. Positive impact from LST assimilation will be greatly enhanced if errors in modeled LST stem primarily from errors in the background model's Bowen ratio that arise *from errors in model soil moisture states*. Prospects for success are much lower if LST errors arise from Bowen ratio errors caused not by soil moisture, but by other errors or weaknesses in LSM physics, such as the ground heat flux errors noted above, or in aerodynamic conductance, as illustrated next. NLDAS investigations uncovered significant differences in simulated LST across the models caused not only by Bowen ratio differences, as expected, but also from surprisingly large inter-model differences in aerodynamic conductance. Figure 7 shows for Jul 99 the multi-station and monthly mean diurnal cycle of ARM-station observed LST and co-located LST simulated from the NLDAS control runs, averaged over the ARM SIRS sites. (The Noah test in Figure 7 is described later.) Mosaic has a mid-day cool bias, as expected, given its high bias in *LE* and *G* and low bias in *H* in Figure 6. VIC and Noah have mid-day warm biases, also as expected, given their low *LE* and high *H* bias in July. While the *sign* of the models' mid-day LST bias in Figure 7 is as expected, the comparative *magnitude* of the bias between the models is perplexing at first, given the *LE* and *H* fluxes in Figure 6. Specifically, the VIC mid-day (19-20 UTC) warm bias in July (about +2 K) is about half as large as Noah (about +4 K), despite VIC's Bowen ratio (*BR* = 2.91) at this time being much higher than Noah's (*BR* = 0.70) and the observed (*BR* = 0.38). Thus, VIC does not yield the largest mid-day warm bias, despite having by far the largest high bias in Bowen ratio. The previously cited high bias in daytime *G* in the Mosaic and VIC control runs does not answer the paradox. ML-N shows that the VIC test of lower surface heat capacity does raise VIC's mid-day LST as expected, but only modestly, still leaving it well below the warmer LST of Noah.

The chief explanation of the paradox of VIC vs. Noah mid-day summer LST lies in striking differences in their aerodynamic conductance (*AC*). Since the LSMs receive *common* surface forcing values of air temperature, wind speed, and surface pressure (and thus air density), then Noah can have higher mid-day values of LST than VIC simultaneously with lower mid-day values of sensible heat flux than VIC if and only if Noah has lower *AC*. Figure 8 depicts monthly-mean diurnal cycle of *AC* for Jul 98 for each LSM control run, averaged across 14 ARM stations. Indeed, the Noah control has substantially smaller daytime *AC* values than Mosaic, and far smaller values than VIC. The low *AC* values in Noah motivated a sensitivity test (denoted by solid squares in Figures 7-8), in which a parameter in Noah's formulation for thermal roughness length was tuned to yield substantially higher *AC*. The mid-day values of *AC* in the Noah test (Figure 8) exceed those of the control by nearly 70%, yielding mid-day values roughly similar to Mosaic, but still notably less than VIC. The LST of this Noah *AC* test in Figure 7 shows a pleasing 2-3 K decrease in Noah's peak daytime LST, cutting Noah's mid-day warm bias by roughly half. Intriguingly, the Noah test and control runs exhibit relatively little change in mid-day sensible heat flux (not shown, see ML-N) -- and thus relatively little change in mid-day latent heat flux -- because the impact of increased *AC* is offset by the smaller difference between the air temperature and now cooler LST. Thus the tuning of the Noah thermal roughness length parameter was successful in substantially reducing Noah's mid-day LST warm bias without degrading the relatively good sensible and latent heat fluxes, and hence this thermal roughness length parameter was adopted as the standard in subsequent Noah runs, such as those in the next section.

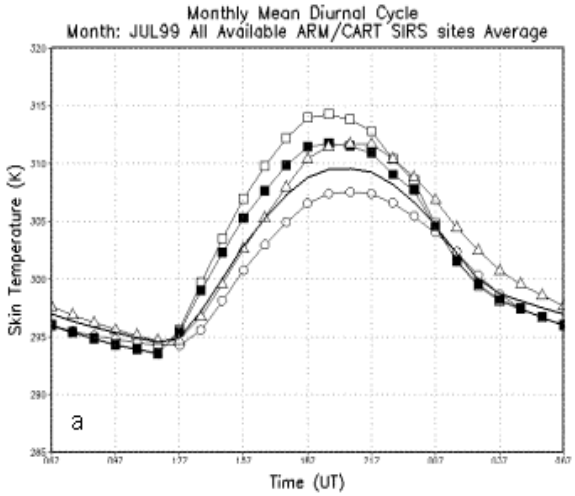

Figure 7 Monthly mean diurnal cycle of LST (K) for Jul 99 averaged over all ARM SIRS sites from observations (no symbols), VIC control (open triangles), Mosaic control (open circles), Noah control (open squares) and Noah test (solid squares).

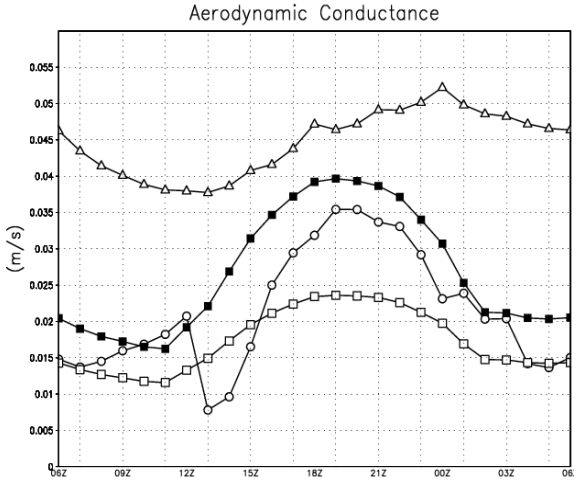

Figure 8 Monthly mean diurnal cycle of aerodynamic conductance (ms-1) for Jul 98 averaged over all ARM SIRS sites for VIC control (open triangles), Mosaic control(open circles), Noah control (open squares) and Noah test (solid squares).

The ARM-station observations of LST are also useful for validating GOES satellite-based retrievals of hourly LST, as a prerequisite for assimilating the latter in the next section. The retrievals here were obtained from GOES-8 via the so-called "split-window" technique, which provided fields of hourly LST at 0.5° spatial resolution in cloud-free conditions during daytime. We bilinearly interpolated the GOES LST fields to the 1/8° NLDAS grid. MN-L and references therein further describe the retrieval technique, the associated cloud screening, and the thermal surface emissivity assumptions. Figure 9 presents the monthly and multi-station mean of the daytime hourly diurnal cycle of observed LST and collocated GOES-8 retrieval LST over 22ARM/SIRS sites for Jul 98 (other months and years are shown in ML-N) at the times when the GOES retrieval detected virtually zero cloud. In Figure 9, the GOES LST reproduces the observed mean diurnal cycle, though it shows a small cool bias in the afternoon (likely from undetected sub-resolution cumulus clouds). ML-N present additional results such as GOES vs. ARM vs. NLDAS LSM LST in station-by-station scatter plots at fixed times of day, and then proceeds to use the GOES LST to validate LSM LST in CONUS regions beyond the ARM network.

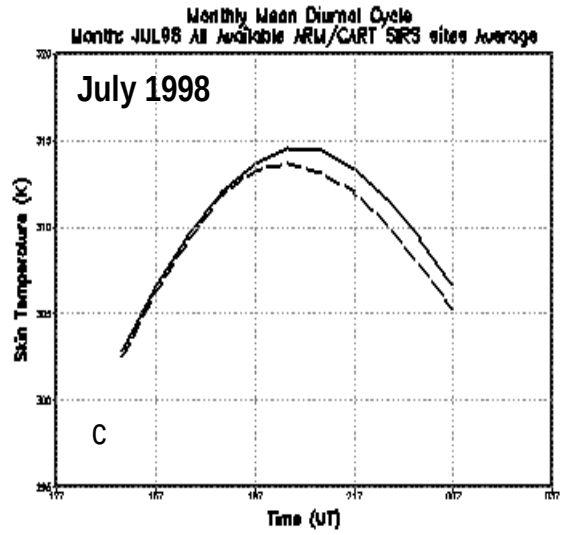

Figure 9 Monthly mean diurnal cycle of LST (K) averaged over ARM SIRS sites for Jul 98 from ARM obs (solid) and GOES-East retrievals (dashed).

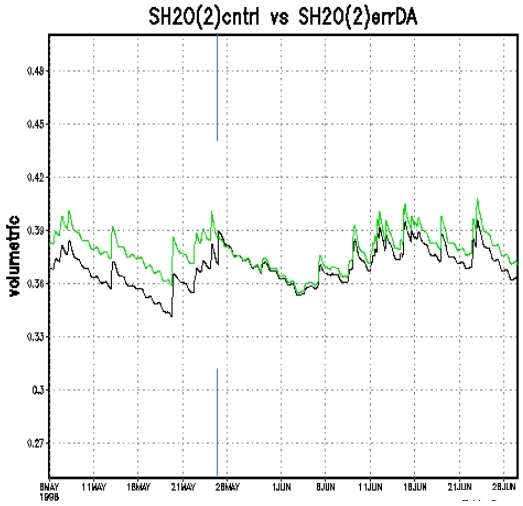

Figure 10 Volumetric soil moisture for Noah soil layer 2 (10-40 cm) for control (top line) and assimilation (lower line) during May-Jun 98.

5. Assimilation of LST in the Noah LSM

Next we present progress at NCEP since the published papers of Section 1 to develop LST assimilation in Noah, via its adjoint / tangent linear model. To test our basic approach, we first performed 1-D identical-twin experiments with the Noah column model for 1998, following a 1997 spin-up year, all forced with 30-minute surface observations at a flux station operated by NOAA/ARL in east central Illinois. Three runs were executed for 1998: 1) the control run, 2) a degraded forcing run in which a 30% reduction was imposed on all moderate or greater amounts of the 30-minute precipitation, and 3) as in 2), but assimilating the simulated LST of the control run for a 3½-day period beginning 0000 UTC on 25 May. Figure 10 shows the Noah layer-2 soil moisture of the control run and the LST 4DDA run for May-Jun 98. The vertical line in Figure 10 denotes the start of the 3½-day assimilation. During this period, the assimilation routine calculates the cost function and the tangent linear of the Noah LSM and finds the optimal correction to the soil moisture state of 0000 UTC on May 25 that minimizes the difference between the "control" and simulated LST over the subsequent 3½ days. There is no assimilation after the 3½ days, so the runs drift apart in June.

We next introduce a highly simplified 4D-Var assimilation of LST. We start with a typical cost function

$$J(x) = (x - x_b)^T B^{-1} (x - x_b) + \sum_{i=1}^{n} (y_i - H_i[x_i])^T R_i^{-1} (y_i - H_i[x_i]) \quad (1)$$

where J is the cost function, x the model state (soil moisture content, SMC), x_b the model background state, B the background error covariance matrix, n the number of observations over the assimilation interval, Y the observed state (LST), H the observation operator (to transform the soil moisture state to LST), and R the error covariance matrix for observation errors. We then apply the following assumptions:

1) For given surface forcing, we assume that LST is mainly a function of SMC, and hence for each assimilation interval, a functional relationship T(SMC) exists, which is the observation operator H.
2) The Noah LSM can be linearized around $x_i = \mathbf{M}_i \mathbf{M}_{i-1} \ldots \mathbf{M}_1 x_1$; its background state can be written as a succession of linear operators $\mathbf{M}_i$.
3) The observation operator can be linearized around a state variable x, and hence

$$y_i - H_i M_{1->i}(x) \cong y_i - H_i M_{1->i}(x_b) - \mathbf{H}_i \mathbf{M}_{1->i}(x - x_b) \quad (2)$$

We then apply these additional simplifying assumptions during each 6-hour mid-day assimilation window:

a) $\mathbf{M}$ = I (the identity matrix), i.e. total evaporation does not change total soil moisture by more than one percent (Note: we do not assimilate if there is precipitation.)
b) $\mathbf{H}i = [d(LST_i)/d(SMC_i)]$, the rate of change of LST with soil moisture is approximately constant during any given day's assimilation interval and is estimated numerically, resulting in an estimate for the 6-hour mean $\bar{\mathbf{H}}$.
c) $\mathbf{B}$, $\mathbf{R}$ = I for the estimation of the cost function with adjusted units. Weighting coefficients are chosen based on empirical evidence of time scales. This leads to the following gradient of the cost function (without the background term):

$$-\tfrac{1}{2}\nabla J(x) = \sum_{i=1}^{n} \mathbf{H}_i^T \left(y_i - H_i M_{1->i} x\right) = \bar{\mathbf{H}}^T \sum_{i=1}^{n} \left(y_i - H_i M_{1->i} x\right) \quad (3)$$

The cost function for the analysis increment has a minimum where the gradient equals zero. Therefore the sum of the differences has to be zero, leading to

$$x_1 = x_b + \frac{\bar{\mathbf{H}}^T}{n} \sum_{i=1}^{n} \left(y_i - H_i M_{1->i} x_b\right) \quad (4)$$

where x_b is the background state at t=1. This is the update equation for the case of perfect measurements and zero background weight. One can set adjustment timescales using fractions of the increment, e.g. 50% here.

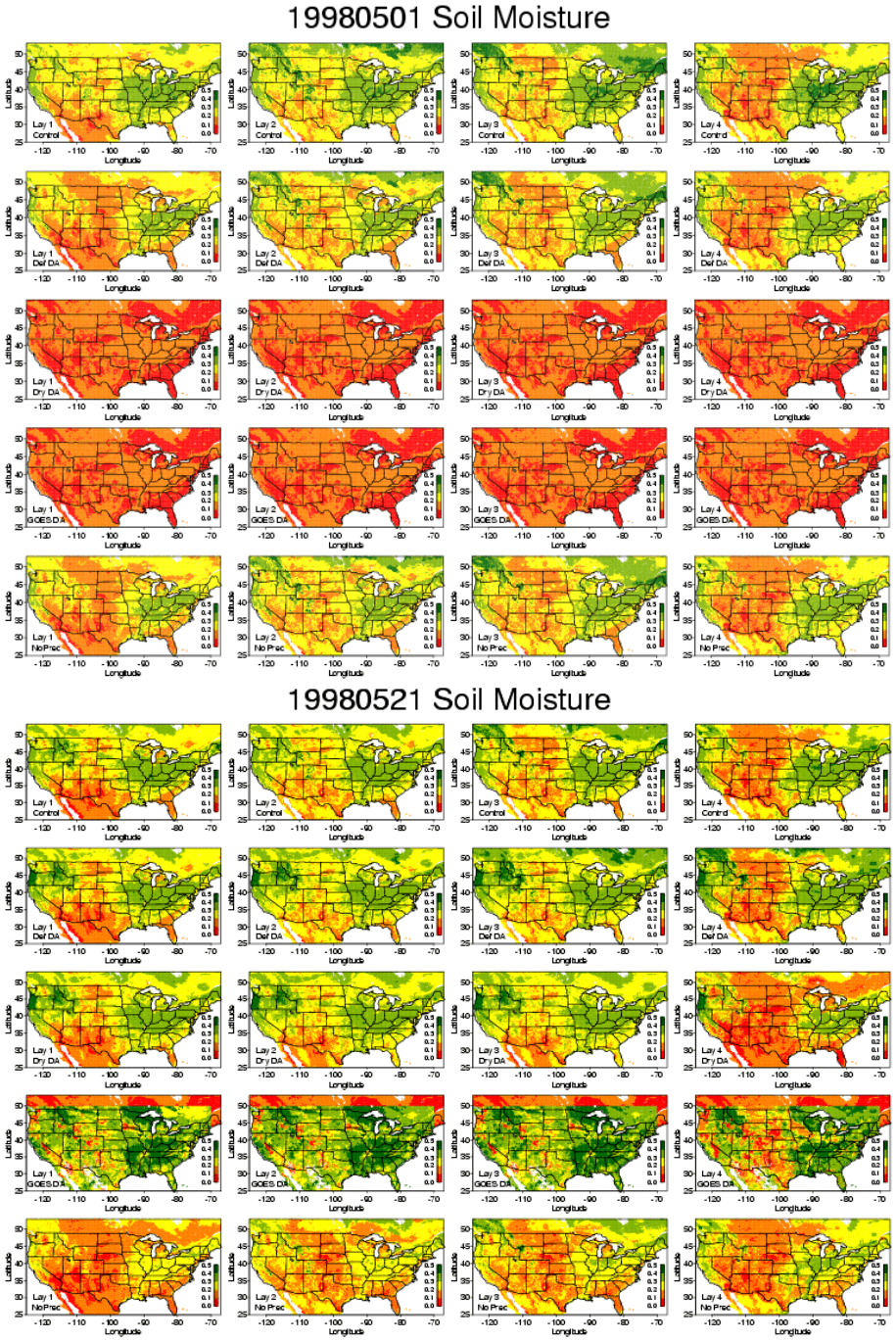

Figure 11 Soil moisture (volumetric) at assimilation-start time of 01 May 98 (top 5 rows) and after three assimilating weeks on 21 May 98 (bottom 5 rows). Left to right, columns 1-4 depict soil layers 1-4 (0-10, 10-40, 40-100, 100-200 cm). In each 5-row set: Row 1 = Control run (no assimilation, no degraded forcing, no degraded initial conditions), Row 5 = Degraded Benchmark run (no assimilation, zero precipitation after 01 March 98), Row 2 = as in Degraded Benchmark, except assimilates LST of Control run as of 01 May and thereafter, Row 3 = as in Row 3, except with added degradation of all soil moisture set to wilting point on 01 May, Row 4 = as in Row 3, except assimilated LST is GOES LST.

This method was used in the Noah LSM to assimilate 1) identical-twin control-run LST and 2) GOES satellite LST over the entire NLDAS CONUS domain during daily, 6-hour mid-day intervals over five months beginning 01 May 98. No soil moisture was assimilated in the bottom soil layer (layer 4, 100-200 cm). We examine the ability of the LST assimilation to overcome two severe degradations that we impose in

the assimilation runs: a) zero precipitation everywhere at all times from 01 May onward and b) initial soil moisture set to wilting point everywhere on 01 May. Additionally, in a second run assimilating control-run LST, we impose less severe but still dry initial conditions on 01 May by taking them from a non-assimilating benchmark run with zero precipitation after 01 Mar 98. Figure 11 presents the results.

Both the top and bottom half of Figure 11 depict five runs in five rows, of which Row 1 is the control, Rows 2, 3, 4 are the three assimilation runs, and Row 5 is a non-assimilating benchmark with zero precipitation. The top half of Figure 11 shows the dry initial states imposed on all three assimilation runs. The bottom half shows how quickly (by three weeks) the assimilating runs recharge (moisten) the dry initial soil states and overcome the zero precipitation forcing. As expected, the two runs assimilating the control-run LST agree most closely with the control run. The run assimilating the GOES LST develops a moist bias compared to the control, likely from the modest cool bias noted in the GOES LST in Figure 9. Future efforts will pursue bias corrections for the GOES LST.

Acknowledgments

The work by NLDAS partners was largely sponsored by the GCIP/GAPP program of the NOAA Office of Global Programs. NASA/GSFC was supported by NASA's Terrestrial Hydrology Program. The U.S. Department of Energy (DOE) provided their data (ARM) free of charge, as did the Illinois Water Survey.

Reference

Mitchell K.E., D. Lohmann, P. R. Houser, E. F. Wood, J. C. Schaake, A. Robock, B. A. Cosgrove, J. Sheffield, Q. Duan, L. Luo, R. W. Higgins, R. T. Pinker, J. D. Tarpley, D. P. Lettenmaier, C. H. Marshall, J. K. Entin, M. Pan, W. Shi, V. Koren, J. Meng, B. H. Ramsay, A. A. Bailey, 2004: The multi-institution North American Land Data Assimilation System (NLDAS): Utilizing multiple GCIP products and partners in a continental distributed hydrological modeling system, *J. Geophys. Res.*, **109**, D07S90, doi:10.1029/2003JD003823.